Charge disproportionation in transition metal oxides

Sadoc, Aymeric Gaël Jocelyn

Chapter 4

Nature of the ground state and the pressure induced spin transition in $CaFeO_3$

Abstract

Ab initio calculations have been performed to clarify the character of the ground state of the high temperature phase of $CaFeO_3$ at different external pressures. The analysis of the correlated N-electron wave function of properly embedded FeO_6 clusters in terms of optimal atomic orbitals clearly establishes the character of the ground state as being dominated by charge transfer configurations. For all pressures, the number of Fe-3d electrons is around 5 and Fe should be considered as a Fe^{3+} ion. We find a S=2 to S=1 transition around 25 GPa in the $CaFeO_3$ crystal.

4.1 Introduction

In this Chapter we use the embedded cluster approach to describe perovskite oxides. Most of the perovskite oxides exhibit charge, orbital and magnetic ordering. [124] For some transition metal oxides that are believed to show charge ordering, the ordering of the charges is still not well understood. This points the interest on $CaFeO_3$, which is, following the ionic model, composed of high valent Fe^{4+} (d^4) Jahn-Teller active ions but shows, instead of JT distortion, an alternative type of distortion interpreted as charge disproportionation at low temperature.

As mentioned in Chapter 1, there exists several type of experimental works that can be

used to understand the physics involved in these crystals. The room temperature and low temperature crystal structures of $CaFeO_3$ have been determined by Woodward *et al.* [4] and Takeda *et al.* [6] using powder diffraction technique. At 300 K the crystal structure is distorted from the ideal perovskite structure by tilting of the octahedra. Below ∼290 K, two distinct Fe signals appear and the symmetry is lowered from the P_{bnm} to the $P_{2_1/n}$ space group. In addition to the tilting of the octahedra, the low temperature structure exhibits two different Fe sites composed of small and large octahedra. Information about the electronic configuration of the Fe ions at the different sites in the low temperature phase was derived from the ^{57}Fe Mössbauer spectrum. [13] The single line found at high temperature is split when the temperature is lowered, which has been interpreted from the two different isomer shift values has been interpreted as arising from a transition as a transition form paramagnetic non-charge-disproportionated phase, containing equivalent Fe^{4+} ions, to a paramagnetic charge-disproportionated (CD) phase containing Fe^{3+} and Fe^{5+} ions (T_{CD}=298 K). A second transition from paramagnetic charge-disproportionated phase (doublet peak) to antiferromagnetic charge disproportionated phase (two sextets peaks - T_{Neel}=115 K) has also been characterized. Moreover, in situ ^{57}Fe Mössbauer spectroscopy and X-ray diffraction under pressure suggested the existence of yet another phase. The two different signals observed for normal and high pressure were interpreted as a pressure induced high spin (HS) to low spin (LS) transition. [14] More recently, the presence of one specific mode in the Raman spectra determined by Ghosh *et al.* [15] was interpreted as a sign that some JT-type distortion is present at room temperature in $CaFeO_3$, indicating the existence of a JT Fe^{4+} (d^4) ionic state along with the non-JT Fe^{3+} state (d^5L^{-1} where L^{-1} denotes a hole on the oxygens ligands).

The $SrFeO_3$ isoelectronic compound has an almost ideal perovskite crystal structure, the Fe–O–Fe angle = 180° compared to the 155° for $CaFeO_3$. This compound does not show any indication of CD for temperatures down to 4 K. [16] Only one iron site is observed among all temperature and pressure variations. Bocquet *et al.* [17] concluded from X-ray and UV photoemission spectroscopy that the ground state of $SrFeO_3$ consists of heavily mixed d^4 and d^5L^{-1} states in agreement with more recent XAS measurements combined with semi-

empirical cluster calculations [18] that emphasize a ground state containing considerable O-2p hole character. Another interesting comparison can be made with $LaMnO_3$ which is also isoelectronic. The Mn^{3+} (d^4) ions show a strong JT distortion at 750 K [125–127] and all metal sites maintain the same effective charge. This different behavior has been interpreted [128] in a way that manganites prefer JT distortion because of the weaker covalent character of the Mn–O bond compared to the Fe–O bond.

The marked differences between the LDA and LDA+U band structure reveal the importance of electron correlation in the electronic structure of $CaFeO_3$. Moreover, these calculations indicate a strong Fe-3d–O-2p mixing. [31] In order to treat these electron correlation effects in a rigorous, *ab initio* way and to quantify the importance of the O-2p to Fe-3d charge transfer effects, we use the embedded cluster approach in combination with state-of-the-art quantum chemical methods. We investigate the character of the ground state at room temperature and normal pressure and also report the evolution of low-lying excited states with increasing pressure. We present in this Chapter the results from embedded cluster calculations has introduced in Section 2.4.

4.2 Details of calculations

The electronic structure of an $[FeO_6]^{8-}$ cluster (see Figure 4.1) is represented as accurate as possible with standard quantum chemical procedures as outlined in Chapter 2. The effect of the rest of the crystal is accounted for by considering an external potential as outlined in equation 2.9 from the term $V_{embedding}$. The ions included in a sphere of 5 Å around the central ion (excluding those already in the basic cluster) are represented with *ab initio* Embedded Model Potentials (AIEMP) [44]. The AIEMPs for Ca, Fe and O in $CaFeO_3$ are optimized following the procedure given in Ref. [45]. For an ideal ionic system the strong orthogonality condition is fulfilled and the bare AIEMPs give an accurate representation of the external ions. However, when the cluster wave function has non-negligible amplitude outside the cluster region, the strong orthogonality condition can only be maintained by adding basis functions to the atoms represented by AIEMPs [49]. In the present work we

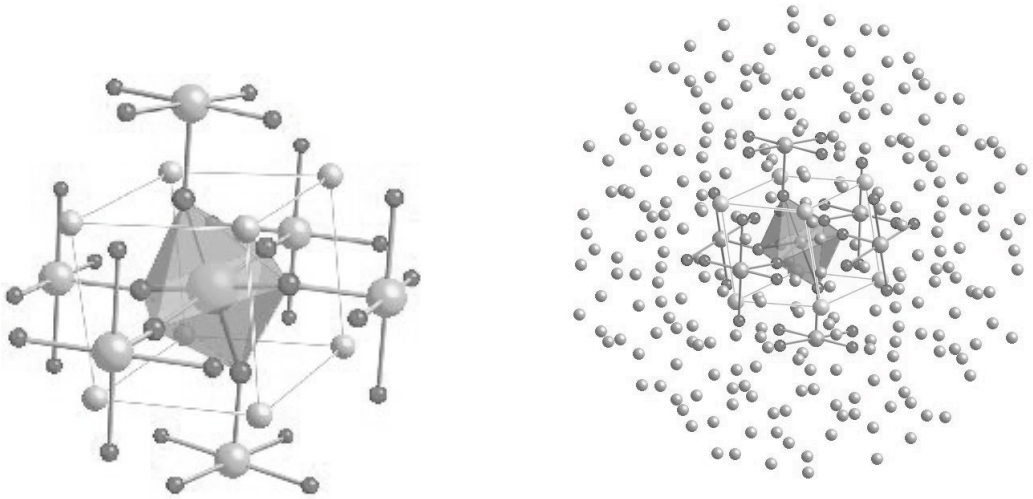

Figure 4.1: *$[FeO_6]^{8-}$ basic cluster embedded in AIEMPs (left) plus the optimized point charges (right)*

add ($1s$,$1p$) valence basis functions to the oxygen and the iron atoms around the basic cluster (AIEMP-sp). In addition, the long-range electrostatic interactions are considered with a set of optimized point charges from the ionic model that reproduce the Madelung field in the cluster region arising from the rest of the crystal. The positions of the atoms in the cluster and its embedding are defined by the crystal structure determination of the room temperature phase by Woodward *et al.* [4]

The one electron basis set employed in the present work to describe the one-electron functions (orbitals) in the cluster region is derived from a ($21s$, $15p$, $10d$, $6f$) primitive basis set for iron and ($14s$, $9p$, $4d$) primitive basis set for oxygen. Following the atomic natural orbital (ANO) contraction of Widmark and co-workers, [77, 78] we use a ($6s$, $5p$, $4d$, $1f$) basis for Fe and a ($4s$, $3p$, $1d$) basis for O.

Two sets of valence orbitals were used for the definition of the active space of the CASSCF wave function. In the first place, we limited the active space to the five orbitals with mainly Fe-$3d$ character and a set of virtual orbitals of the same symmetry character. Results referring to this active space will be marked with CAS(4,10). The first number indicates the number of active electrons and the second the number of active orbitals. The

Table 4.1: *$CaFeO_3$ lattice parameters and average Fe-O distance in Å with increasing pressure. The parameters are deduced from Ref [4] for 0.1 GPa and Fig. 2 in Ref [14] for larger pressure.*

	0.1 GPa	10 GPa	20 GPa	30 GPa	40 GPa	50 GPa
a	5.31744	5.24673	5.17602	5.09117	5.16195	5.16100
b	5.31744	5.24673	5.17602	5.09117	4.89325	4.83668
c	7.52000	7.42000	7.32000	7.20000	7.20010	7.09000
Fe-O	1.918	1.889	1.865	1.833	1.819	1.803

second active space extends the first one with two occupied orbitals of e_g-like symmetry with mainly O-2p character. The resulting active space is labeled with CAS(8,12). This choice of active space ensures a balanced and unbiased treatment of the most important electronic configurations: the non charge transfer (NCT) Fe-3d^4, the charge transfer (CT) Fe-3$d^5\mathrm{L}^{-1}$, and the double CT (DCT) Fe-3$d^6\mathrm{L}^{-2}$ configuration.

Since the deviations from a perfect octahedral coordination around the Fe ions are small, the deviations from octahedral level splittings are also small. Thus we will denote for clarity the states by their Russell Saunders symbols in the case of O_h site symmetry. The eight lowest lying electronic states were studied: $^5\mathrm{E}_g$, $^5\mathrm{T}_{2g}$, a$^3\mathrm{T}_{1g}$, $^3\mathrm{E}_g$, b$^3\mathrm{T}_{1g}$, $^3\mathrm{T}_{2g}$, $^1\mathrm{T}_{2g}$ and $^1\mathrm{E}_g$. The excitation energies will be related to the $^5\mathrm{E}_g$ ground state unless stated otherwise. All the calculations were done in the C_i symmetry for the $[\mathrm{FeO}_6]^{8-}$ cluster.

Provided that the active space is flexible enough to account for all important non-dynamical electron correlation, CASSCF gives reasonably accurate electron distributions. It, however, fails to reproduce the correct relative energies of the different electronic states due to the lack of dynamical electron correlation effects. These largely atomic effects can efficiently be included in the wave function with complete active space second-order perturbation theory (CASPT2). [54, 55] All CASPT2 calculations were done with an imaginary shift of 0.3 Hartree to avoid the presence of intruder states. [56] All electrons are correlated except those in the Fe-1s, 2s, 2p and O-1s core orbitals. Both scalar relativistic effects and spin-orbit coupling effects are expected to be small and were not considered in the calculations.

Table 4.2: *Relative energies (in eV) of the low-lying electronic states in the embedded FeO_6 cluster to model $CaFeO_3$ at 298 K and ambient pressure. Results are compared at the CAS(4,10)SCF, CAS(8,12)SCF and the subsequent CASPT2 level. The lattice parameters are taken from Ref [4].*

State	Dominant electronic configuration	CAS(4,10)SCF	CAS(8,12)SCF	CASPT2
^5E_g	$e_g^4\ t_{2g}^{*3}\ e_g^{*1}$	0.00 ; 0.06	0.00[1] ; 0.05	0.00 ; 0.04
a^3T_{1g}	$e_g^4\ t_{2g}^{*4}\ e_g^{*0}$	0.61 ; 0.63 ; 0.68	0.24 ; 0.27 ; 0.30	0.46 ; 0.50 ; 0.52
$^1T_{2g}$	$e_g^4\ t_{2g}^{*4}\ e_g^{*0}$	2.23 ; 2.26 ; 2.29	2.04 ; 2.07 ; 2.11	1.98 ; 1.99 ; 2.02
^1E_g	”	2.45 ; 2.48	2.21 ; 2.24	2.16 ; 2.19
^3E_g	$e_g^4\ t_{2g}^{*3}\ e_g^{*1}$	2.54 ; 2.59	2.64 ; 2.69	2.26 ; 2.30
b^3T_{1g}	”	3.06 ; 3.09 ; 3.10	3.42 ; 3.45 ; 3.47	2.72 ; 2.72 ; 2.74
$^3T_{2g}$	”	3.19 ; 3.20 ; 3.23	3.52 ; 3.54 ; 3.57	2.82 ; 2.82 ; 2.82
$^5T_{2g}$	$e_g^4\ t_{2g}^{*2}\ e_g^{*2}$	2.84 ; 2.86 ; 2.86	4.28 ; 4.29 ; 4.32	3.42 ; 3.43 ; 3.47

The effect of the external pressure is simulated by changing the inter atomic distances in the cluster and the embedding, following closely the changes in lattice parameters reported by Takano and co-workers, [14] see Table 4.1. We evaluate the CASPT2 energies of the excited states relative to the ground state at the different pressures using the CAS(8,12) wave function as reference wave function for the perturbational treatment.

4.3 Results and discussion

The two components of the ^5E_g ground state are almost degenerate in all calculations. The distortion of the octahedral surrounding of the Fe ions is too small to induce a preference between occupying one of the two e_g^* orbitals in the $e_g^4\ t_{2g}^{*3}\ e_g^{*1}$ electronic configuration, see Table 4.2. For clarity the inactive orbitals from a CAS(8,12)SCF are omitted from the notations of the electronic configurations. The t_{2g}^* and e_g^* are antibonding linear combinations of Fe-3d and O-2p basis functions, the e_g orbitals are the bonding counterparts of e_g^*. Fig. 4.2 gives a graphical representation of the orbitals of e_g symmetry and Table 4.3 gives a more quantitative account of the character of the orbitals by means of a Mulliken orbital population analysis.

Although the ordering of the different excited states, apart form the $^5T_{2g}$ state, is similar in the CAS(4,10) and CAS(8,12) calculation, the effect of extending the active space with the two e_g orbitals of mainly O-2p_σ character is much more pronounced than in the case of simpler TM-oxides like NiO and CoO. [33, 129] The total CASSCF energy of the ^5E_g state is lowered by approximately 2.5 eV by including the charge transfer configurations in the active space, whereas a lowering of not more than 0.2 eV was found in the case of NiO. Furthermore, we observe significant changes in the relative energies. All the states with dominant $e_g^4\ t_{2g}^{*3}\ e_g^{*1}$ configurations are stabilized by 2.2 - 2.5 eV as the ^5E_g ground state. The states with a dominant $e_g^4\ t_{2g}^{*4}\ e_g^{*0}$ configurations are stabilized by 2.5 - 3.0 eV. The most striking difference is the raise of the relative energy of the $^5T_{2g}$ state from 2.84 eV to 4.28 eV due to a weaker stabilization by 1.16 eV.

In a simple ionic picture the ^5E_g - $^5T_{2g}$ energy difference would correspond to the *ab initio* estimate of Δ in the Racah parametrization scheme. The covalent interactions are, however, so strong that the appropriateness of this simple model is questionable and we prefer to speak here about the $t_{2g}^* - e_g^*$ splitting. Table 4.3 shows a transfer of about 0.2 electron from the e_g to the e_g^* orbitals upon the extension of the active space with the e_g orbitals. On the other hand, the occupation of the t_{2g}^* orbitals remains 3.00 indicating that all charge transfer occurs within the orbitals of e_g symmetry. This flow of electrons (de-)stabilizes the (anti-)bonding orbitals. Since the extension of the active space hardly affects the t_{2g}^* orbitals, the transition from the ^5E_g state to the $^5T_{2g}$ state, in which one electron is transferred from the t_{2g}^* orbital to the e_g^* orbital, becomes energetically less favorable.

The effect of the bonding t_{2g} orbitals with mostly O-2p character is smaller. Therefore, we do not treat these excitations in the CASSCF but their effect is estimated with second-order perturbation theory (CASPT2). Due to symmetry, these excitations have a smaller interaction with the ^5E_g state than with the $^5T_{2g}$ state, the $t_{2g}^* - e_g^*$ splitting is decreased again, giving our final estimate of 3.4 eV. The electron correlation accounted for by CASPT2 increases the splitting of the two lowest states, ^5E_g and a^3T_{1g}, to 0.5 eV.

Table 4.3: *Character of the active orbitals in the CAS(4,10)SCF and CAS(8,12)SCF calculation determined by Mulliken Gross population analysis*

	CAS(4,10)			CAS(8,12)		
Orbital	Occ. Number	Fe-3d	O-2p	Occ. Number	Fe-3d	O-2p
e_g	4.00	–	–	3.80	0.33	0.67
t^*_{2g}	3.00	0.96	0.04	3.00	0.97	0.03
e^*_g	1.00	0.74	0.26	1.20	0.67	0.33

4.3.1 Character of the ground state

The interpretation of the cluster wave function in terms of NCT (Fe-3d^4) and CT (Fe-3$d^5\underline{L}^{-1}$) determinants is not straightforward since the information on covalency is contained in two different places in the multiconfigurational wave function (see Section 2.5). First in the orbitals, which have a mixed character with important contributions from the Fe-3d and O-2p basis functions as can be seen in the population analysis resumed in Table 4.3. Secondly, in the CI expansion of the wave function, where the different electronic configurations (NCT, CT, DCT, etc.) appear with different weights.

Since the choice of the orbitals to express the N-electron CASSCF wave function is not unique, it is possible to establish more clearly the importance of charge transfer in this system by performing a transformation of the orbitals. The analysis of Cooper *et al.* [73, 74] and the CASVB approach of Hirao *et al.* [75] involve transformations amongst all active orbitals, allowing one to interpret the CASSCF wave function in term of valence bond structures. Both approaches lead to an interpretation in terms of non-orthogonal localized orbitals [73, 74] or non-orthogonal spin-functions [75]. In this study we simply rotate pairs of orbitals in the active space in order to minimize the mixing of Fe-3d and O-2p basis functions in the orbitals (see Section 2.5). Figure 4.3 shows the obtained atomic-like orbitals after transformation of the natural orbitals. After re-expressing the CI expansion of the wave function in terms of the atomic-like orbitals the information on the covalence is entirely concentrated in the wave function expansion. The length of the CI expansion for the CAS(8,12)SCF quintet wave function is 60 984 determinants. Summing up the

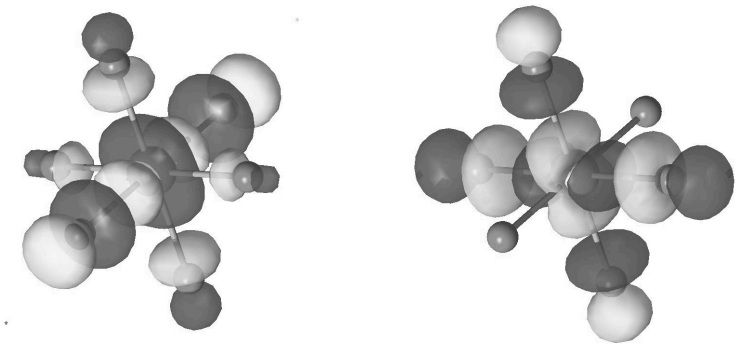

Antibonding natural e_g^* orbitals (mainly Fe-3d)

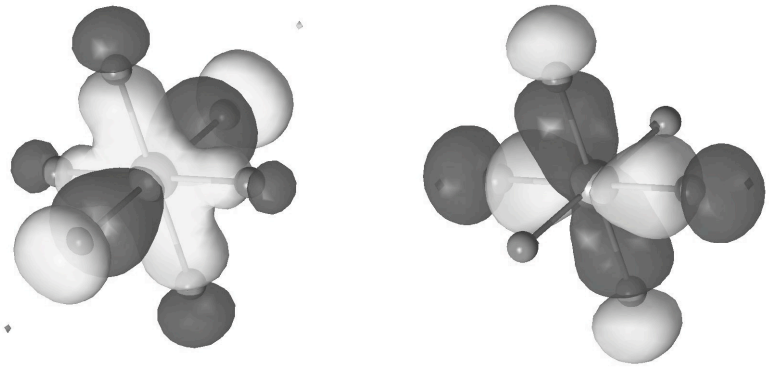

Bonding natural e_g orbitals (mainly O-2p)

Figure 4.2: *Bonding and antibonding CAS(8,12) natural e_g-like orbitals for the [FeO_6]$^{8-}$ cluster embedded in AIEMP-sp and fitted point charges.*

squared coefficients of all the determinants with 4, 3, 2 or 1 electron(s) in the O centered atomic-like orbitals, the ^5E_g ground state can be schematically written as

18.9% NCT + 66.2% CT + 14.0% DCT + 0.4% TCT + ...

This analysis provides theoretical evidence that the ground state is dominated by the Fe-3$d^5\underline{L}^{-1}$ electronic configuration where the 5 d-electrons are mainly coupled to $^6A_{1g}$. This leading configuration is only weakly Jahn-Teller active, and hence, can explain why no JT distortion is observed in $CaFeO_3$ for the room temperature and why the material prefers to go through charge disproportionation while maintaining the octahedral symmetry. The high formal charge of Fe may also give rise to CT from O-2p_π orbitals of t_{2g} symmetry. However, because the interaction between Fe 3d(t_{2g}) and O-2p_π is quite weak, the t_{2g}

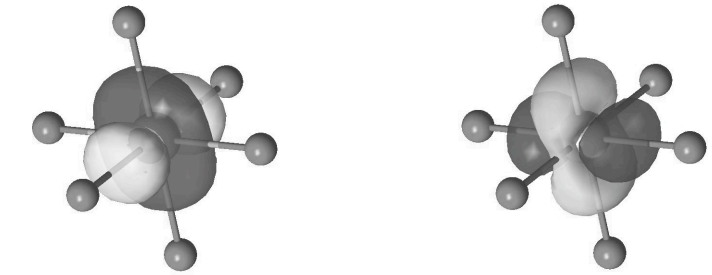

Fe centered e_g orbitals

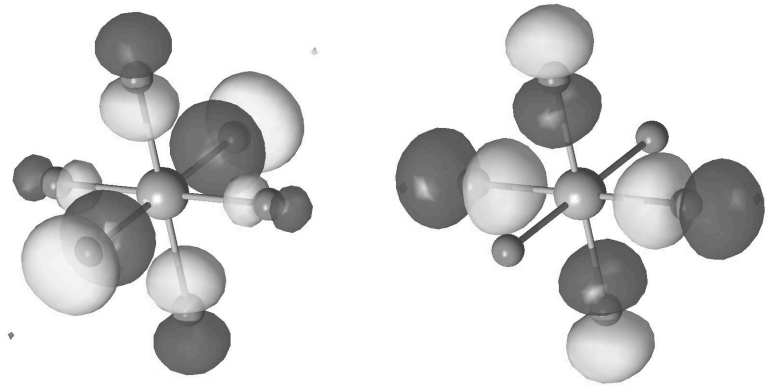

O centered e_g orbitals

Figure 4.3: *Optimal atomic e_g like orbitals obtained from a unitary transformation of the CAS(8,12) natural orbitals of the $[FeO_6]^{8-}$ cluster embedded in AIEMP-sp and fitted point charges.*

orbitals are already essentially O-$2p_\pi$ orbitals and the t_{2g}^* orbitals are already almost pure Fe 3d orbitals. A rotation amongst these orbitals would slightly lower the weight of the NCT configuration. Notice that the embedding of the FeO_6 cluster is constructed using Fe^{4+} and O^{2-} ions. This means that the external potential could bias the NCT (Fe-$3d^4$–O-$2p^6$) configuration. Hence, the weight of 18.9% should be considered as an upper estimate.

4.3.2 Influence of pressure

We proceed with the scheme described in Chapter 2 by using AIEMPs with s and p functions for the first shell of atoms around our cluster and a set of point charges using the lattice parameters reported by Takano *et al.* [14]. Figure 4.4 shows the evolution of

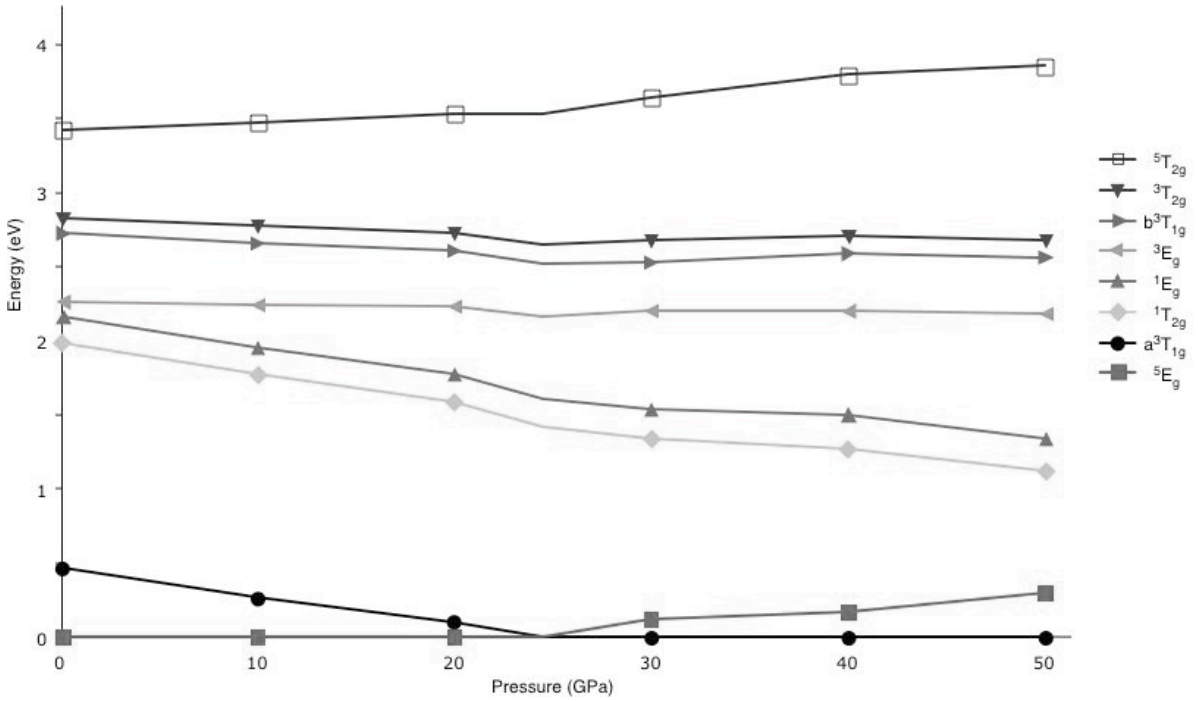

Figure 4.4: *Evolution of the CASPT2 energies with pressure. The lines connecting the markers are a guide to the eyes.*

the relative energies at the CASPT2 level of the different states by increasing the pressure. The ground state energy is taken as reference energy.

The CASPT2 energies follow closely the Tanabe-Sugano diagram for a d^4 ion in octahedral symmetry (see Figure 2.2). [22] This shows that the simple ionic model is a useful ansatz to explain the relative energies, provided that all relevant electronic effects are taken into account. In the Tanabe-Sugano diagrams this is accomplished via parametrization of the B/C and Δ values. In our CASPT2 approach these effects are included via the orbital delocalization and excited configurations. The energies form a smooth curve between 0 and 20 GPa, as can be expected from the gradual reduction of the lattice parameters a=b and c in this pressure range (see Table 4.1). At ≈25 GPa the ligand field is strong enough to induce a spin crossing. The a^3T_{1g} state becomes the ground state of the system. This result is in reasonable agreement with the Mössbauer study realized by Takano *et al.* [14] who measured a pressure induced spin transition at 30 GPa. The energies at 40 and 50 GPa, where the a and b lattice parameters are no longer equal, do not form a smooth con-

Table 4.4: *Evolution of the weights in % of the various VB configurations and number of Fe-d electrons (d-count) as a function of the pressure (in GPa) for the* ^5E_g *and* a^3T_{1g} *states.*

	Pressure	NCT	CT	DCT	TCT	d-count
^5E_g	0.1	18.9	66.2	14.0	0.4	4.93
	10	21.1	64.1	13.7	0.4	4.90
	20	22.3	62.6	14.0	0.4	4.89
	30	23.6	61.0	14.3	0.5	4.89
	40	20.5	60.4	18.6	0.9	4.96
	50	22.9	60.1	15.8	0.7	4.92
a^3T_{1g}	0.1	12.7	55.4	28.4	2.0	5.12
	10	13.8	54.9	27.6	2.1	5.10
	20	14.5	54.5	27.2	2.2	5.09
	30	15.3	53.7	27.0	2.4	5.09
	40	15.3	53.3	27.3	2.5	5.09
	50	13.1	51.1	30.5	3.7	5.17

tinuation of the energies for lower pressures but we do see the same trends for increasing pressure.

We also investigate the evolution of the character of the ^5E_g and a^3T_{1g} wave functions with pressure by performing the same unitary transformation on the orbitals as used previously. Table 4.4 shows the weights of the various configurations as a function of pressure. The CT character of the wave function (defined as the sum of the weights of the CT, DCT and TCT configurations) decreases continuously with increasing pressure for the ^5E_g state up to the phase transition around 30 GPa. This decrease is a consequence of the destabilization of the Fe-3$d(e_g)$ orbitals due to increased ligand field. The abrupt change in the structure at the phase transition causes a discontinuity in this tendency but the CT character decreases again from 40 to 50 GPa. Furthermore, we observe a weaker contribution of NCT configurations in the a^3T_{1g} than in the ^5E_g state. As for the ^5E_g state, the charge transfer for the a^3T_{1g} occurs only within the orbitals of e_g symmetry. The occupation of the t^*_{2g} orbitals remains 4.00. The CT character is stronger in the triplet state because the Fe-3$d(e_g)$ shell is empty in the NCT configuration, whereas it is occupied with one electron for the quintet state.

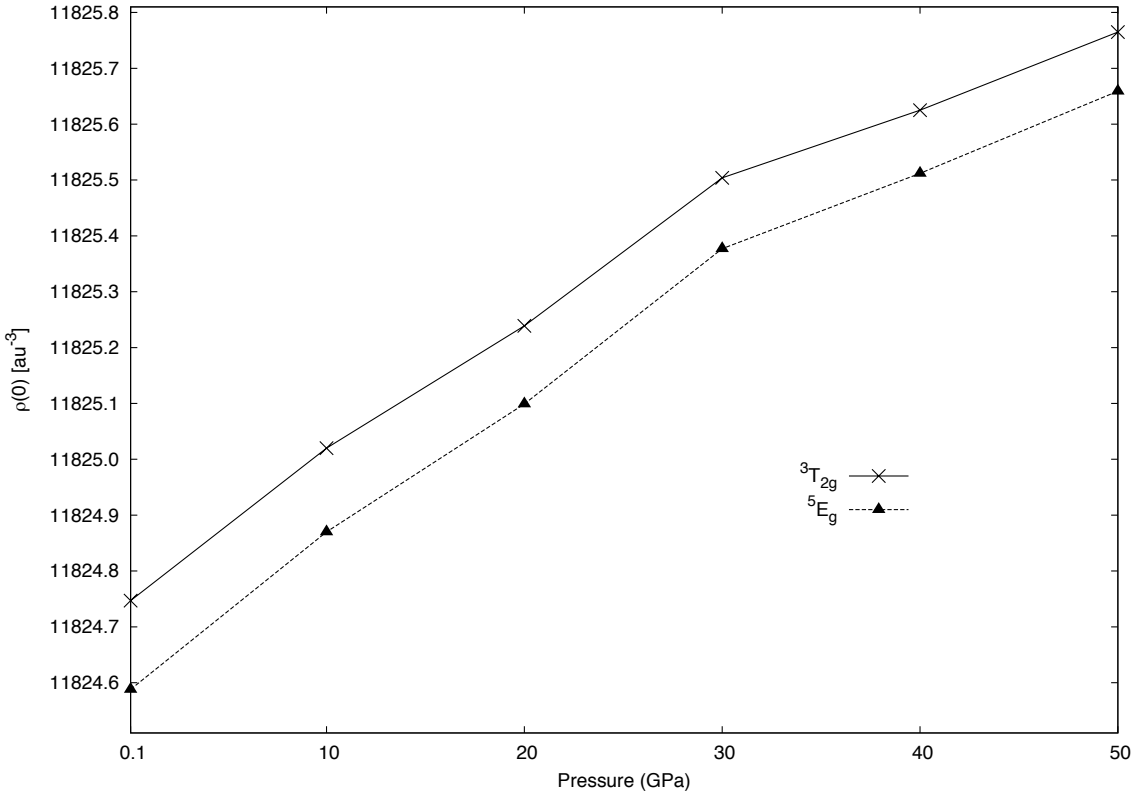

Figure 4.5: *Evolution of the CASSCF density at the Fe nucleus with pressure. The lines connecting the markers are a guide to the eyes.*

Following the work reported in chapter 3 we investigated the evolution of the density at the Fe nucleus with increasing pressure. Figure 4.5 reports the densities at the Fe nucleus calculated with CASSCF wave function method for an increasing pressure. An increase of pressure leads to a logical higher density at the Fe nucleus. The triplet state has a higher density than the quintet ground state, which seems also logical due to the more compact character of the electron clouds when electrons are located in the more compact t_{2g} orbitals. This finding is in perfect agreement with the experiment which reports a drop of 0.25 mm/s for the IS value from Mössbauer spectroscopy. Using the calibration curve reported before we calculate a drop of 0.127 au^3 in the density at 30 GPa leading to an estimated value of 0.04 mm/s for the IS.

4.4 Conclusions

The crystal field model predicts a ^5E_g(Fe-t_{2g}^3 e_g^1) ground state for the $[FeO_6]^{8-}$ octahedron for the high-temperature $CaFeO_3$ crystal structure. Our CAS(4,10)SCF calculations confirm such a ground state with important Fe-3d–O-2p mixing in the e_g shell as in ligand field theory. We find a e_g^4 t_{2g}^{*3} e_g^{*1} electronic configuration with 25% O-2p contribution to the antibonding e_g^* orbital. Extension of the active space with the bonding e_g orbitals not only introduces CT configurations in the wave function expansion but also enhances the O-2p–Fe-3d mixing from one quarter to one third. Both effects lead to a stronger contribution of Fe-3d^5 configurations. Using this bonding–antibonding orbital set, this increase in the covalency is not easily quantified. However, expressing the wave function in optimal atomic-like orbitals reveals that the leading configuration in the ^5E_g ground state wave function is O-2p(e_g^3)Fe-3d(t_{2g}^3 e_g^2). The number of Fe-3d electrons is close to five, and hence, Fe in the high temperature phase of $CaFeO_3$ has to be considered as an Fe^{3+} ion.

The pressure dependence of the CASPT2 energies of the lowest electronic states leads to a spin transition, as seen in Mössbauer spectroscopy. Between 20 and 30 GPa the ground state changes from ^5E_g to a^3T_{1g}. We note that our CASPT2 approach is known to slightly overestimate the energies of high spin states. [130] Our estimate is that a more accurate account of the electron correlation effects will lower the a^3T_{1g} with respect to the ^5E_g, leading to a spin transition around 20 GPa. In the whole pressure range, the number of Fe-3d electrons is around 5. The quintet state is dominated by the CT configuration with important, almost equal contributions from the NCT and DCT configurations. For the triplet state, the NCT is less important and the DCT becomes twice as important compared to the ^5E_g state.

The present study concerns the high-temperature structure of $CaFeO_3$. Below 290 K the structure is $P2_1/n$, containing alternating large and small FeO_6 octahedra. Charge disproportionation is assumed, but there is no generally accepted picture of the electronic structure. The geometry of the small octahedron is close to that of 20 GPa. We find for this geometry that the high spin ^5E_g and low spin a^3T_{1g} states are very close in energy. A

more detailed study of the low temperature phase electronic structure is developed Chapter 6.